Effect of Flow Divergence on the Structure of Detonation in Rich H_2-NO_2/N_2O_4 Mixtures

Behrang Shirvani[1], Zihang Ni [2], Fernando Veiga-López[3], Brian Maxwell[1], Rémy Mével[4], Jocelyn Luche[5], Pierre Vidal[5]

[1]Department of Mechanical Engineering, University of Ottawa, 161 Louis Pasteur, Ottawa, K1N 6N5, Canada

[2]School of Aerospace Engineering, Tsinghua University, Beijing, China

[3]Aerolab, Instituto de Física e Ciencias Aeroespaciais (IFCAE), Universidade de Vigo, Ourense, Galicia, España

[4]School of Aeronautics and Astronautics, Zhejiang University, Hangzhou, China

[5] Institut Pprime, UPR 3346 CNRS, Fluid, Thermal and Combustion Sciences Department, ENSMA, Téléport 2, 1 Av. Clément Ader, Chasseneuil-du-Poitou, France

1 Introduction

Detonation in rich H_2-NO_2/N_2O_4 mixtures demonstrate the particularity of being driven by two successive stages of heat release of very different amplitude and characteristic time scale [1]. This particular feature results in the formation of a detonation with a double cellular structure, whose propagation has been studied both experimentally and numerically. Experimentally, such a complex structure has been observed for H_2-NO_2/N_2O_4 mixtures in several studies. Joubert et al. [1] studied the propagation of detonation in H_2-NO_2/N_2O_4 mixtures over a range of equivalence ratios from Φ=0.5-2 and for initial pressures from 100-200 kPa using the soot foil technique. Luche et al. [2] employed Ar-diluted mixtures with Φ=1.2. They also applied the soot foil technique for Ar dilution of up to 60%. In both studies by Joubert et al. and Luche et al., the double cellular structure can be unambiguously identified for the rich mixtures under most of the conditions investigated. Numerically, several studies were also performed. Guilly et al. [3] carried out a detailed parametric study using a two-step chemical model and showed that there are critical conditions for the existence of the double cellular structure. Sugiyama and Matsuo [4] employed an approach similar to that used by Guilly et al. and showed that a double cellular structure detonation can be divided into a primary and a secondary detonation. Davidenko et al. [5] were the first to perform a numerical simulation of a double cellular structure using a reduced chemical model instead of a globalized one. They confirmed that the existence of such a structure is correlated with the existence of two stages of heat release with very different characteristics.

In addition to the double cell structure, the near-limit behavior of detonation in H_2-NO_2/N_2O_4 mixtures is also very particular and unique. For instance, Luche et al. [2] reported that for a Ar dilution above 50%, the double cellular structure disappears and a low-velocity detonation (LVD) with single cellular structure is observed. In this case, it was suspected that the exothermic heat released associated with the second stage was pushed beyond the sonic surface, giving rise to a lower than expected detonation velocity. LVD thus refers to the detonation speed influenced only by the first stage of heat release [2]. Such a behavior was also reported by Desbordes et al. [6] but for very lean H_2-NO_2/N_2O_4 mixtures. The near-limit behavior of detonation in H_2-NO_2/N_2O_4 mixtures has been further studied by Virot et al. [7]. They used rich mixtures, at Φ=1.2, with and without Ar dilution and progressively decreased the initial pressure, keeping all other parameter constant. At a critical pressure, either a high- or a low-velocity detonation can be observed for successive experiments with same conditions. Above this initial pressure, the velocity is consistent within few percent with the theoretical Chapman-Jouguet velocity (D_{CJ}) and the double structure is always observed. Below this initial pressure, the velocity deficit becomes larger than 15%, and can reach almost 30% as pressure is further decreased. In addition, a single

Correspondence to: bmaxwell@uottawa.ca

cellular was reported. In the study of Virot et al. [7], two-dimensional numerical simulations were also performed using a Reduced reaction mechanism with two stages of heat release. When these two stages were of the same amplitude, a double cellular structure was obtained. On the other hand, when the second stage of heat release was decreased to zero to mimic various losses at the wall, a LVD with a single dominant cell width was obtained. Thus, LVD regimes could be studied using curved detonation models, e.g., [8, 9], because the curvature of the leading shock results from the lateral expansion of the flow. Indeed, the front of the expansion wave – the "sonic locus" – penetrates deeper into the reaction zone, i.e., closer to the leading shock, as the expansion rate increases relative to that of the heat release. Eventually, the detonation regime shifts from quasi-CJ regimes to LVD regimes when the position of the sonic locus is smaller than that of the last stage(s) of heat release. Examples include the tube diameter effect on the detonation of some granular explosives, with quasi-CJ regimes at large tube diameters and LVD at smaller diameters [10], and the two LVD regimes resulting from incomplete nucleosynthesis for the model astrophysical plasma 50% C + 50% O [11].

The main objective of the present study was to obtain more information on the existence of low-speed detonation in H_2-NO_2/N_2O_4 mixtures. To achieve this goal, we have examined the dynamics of curved detonation in these mixtures using a weakly-curved detonation approach as well as two-dimensional unsteady numerical simulations which incorporate a flow divergence based boundary layer model following the methodology outlined by Smith et al. [12].

2 Weakly-curved detonation structure

The flow is described by the steady reactive Euler equations including a boundary layer (BL) loss term

$$\frac{\mathrm{d}\rho}{\mathrm{d}x} = -\frac{\rho}{u}\frac{(\dot{\sigma} - M^2\dot{\sigma}_A)}{\eta}, \quad \frac{\mathrm{d}u}{\mathrm{d}x} = \frac{(\dot{\sigma} - \dot{\sigma}_A)}{\eta}, \quad \frac{\mathrm{d}P}{\mathrm{d}x} = -\rho u\frac{(\dot{\sigma} - \dot{\sigma}_A)}{\eta}, \quad \frac{\mathrm{d}Y_i}{\mathrm{d}x} = W_i\frac{\dot{\omega}_i}{\rho u} \tag{1}$$

where ρ, u, P, and x are the mixture density, axial velocity in the wave-attached frame, pressure, and relative position to the shock, respectively. The mass fraction, molecular weight and net production/consumption rate per unit mass of species i are given by Y_i, W_i and $\dot{\omega}_i$. The sonic parameter η is defined as $\eta = 1 - M^2$ where M is the Mach number relative to the leading shock. $\dot{\sigma}$ is the thermicity and $\dot{\sigma}_A$ represent the losses induced by the boundary layer in a tube [9], reading:

$$\dot{\sigma}_A = u\frac{2}{r + \delta^*(x)}\frac{\mathrm{d}\delta^*(x)}{\mathrm{d}x}, \tag{2}$$

where r is the radius of the tube and $\delta^*(x)$ is the boundary-layer-induced displacement thickness. For a laminar boundary layer, $\delta^*(x)$ is given by [13]

$$\delta^*(x) = K_M\sqrt{\nu_s\int_0^x \frac{1}{u(x)}\mathrm{d}x}, \tag{3}$$

where ν_s is the post-shock kinetic viscosity, and $K_M = 4.5$ is the Mirel's constant.

Figure 1 a) shows the evolution of the velocity with initial pressure. The weakly-curved model predicts a dramatic drop in velocity as P_0 reaches approximately 10 kPa. In contrast, the experimental data demonstrate the existence of two branches, respectively located in the high- and low-velocity regimes. In the high-velocity regime, the experimental and computed velocities are consistent with each other. On the other hand, the weakly-curved model fails in predicting the low-velocity branch. Figure 1 b) shows the corresponding the temperature profiles at different P_0. Lowering the initial pressure induces

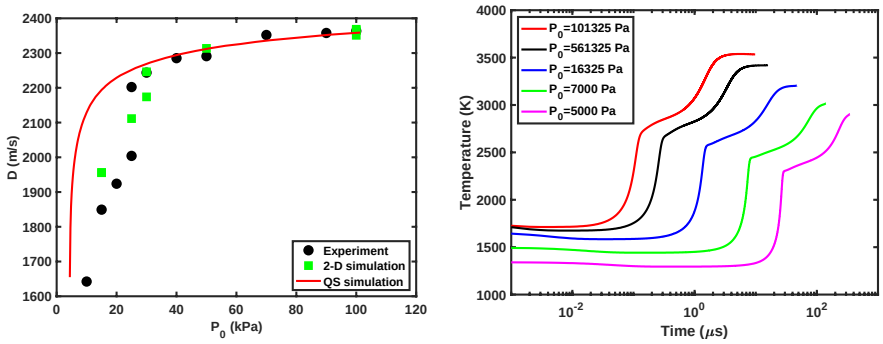

Figure 1: a) Experimental [7] and numerical detonation velocity as a function of P_0 and b) example temperature profiles for H_2-NO_2/N_2O_4 mixtures with Φ=1.2. The numerical values were obtained with the weakly-curved detonation model considering a laminar boundary layer. $T_0 = 300$ K.

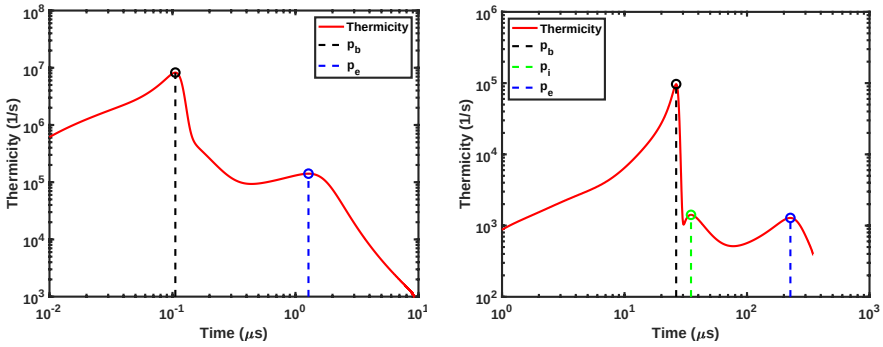

a) $P_0 = 101325$ Pa b) $P_0 = 5000$ Pa

Figure 2: Thermicity profiles calculated with the weakly-curved detonation model at a) highss-pressure and b) low-pressure for rich H_2-NO_2/N_2O_4(-Ar) mixture with Φ=1.2. $T_0 = 300$ K.

the progressive increase of the induction zone length associated with the first step of heat release. In addition, the sonic point penetrates further and further into the reaction zone, which progressively weakens the second step of heat release. It should be noted that the sonic point is easily determined by the temperature profiles shown in Figure 1 b), since the ZND computation ends before the $M \rightarrow 1$ singularity to avoid computational difficulties [14]. Figure 2 shows the thermicity profiles calculated under high- and low-pressure conditions. For near-ideal detonation propagation, i.e., the high-pressure case, we observed two peaks of thermicity, which is consistent with previous ZND calculations for rich H_2-NO_2/N_2O_4 mixtures. In contrast, examination of the thermicity profile obtained at low pressure reveals that three peaks of heat release exist under these conditions. The first peak, noted P_b, is several orders of magnitude higher than the two others, which have similar heights. The intermediate peak, P_i, is located at a short distance from the first peak, while the third peak, noted P_e, is located at a much longer distance. To gain further insight into the origin of the unusual heat release profile observed at low pressure, we have computed the heat release rate (HRR) per reaction, see Figure 3. The first peak, P_b, is mainly attributed to the sequence NO_2+H=NO+OH followed by H_2+OH=H_2O+H, while the third peak, P_e is due to the reduction of NO: NO+N=N_2+O. These results are consistent with the analysis in [5]. The appearance of the second peak, P_i is attributed to the increased contribution to the total HRR of the two reactions HNO+M=H+NO+M and HNO+H=NO+H_2.

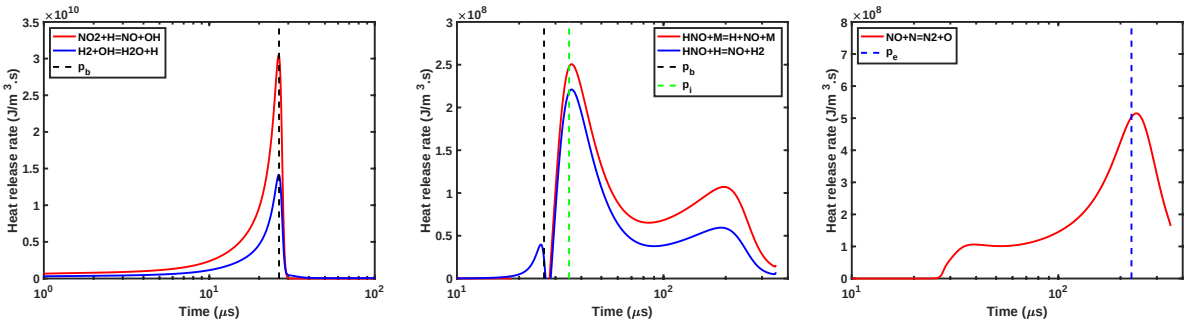

a) Beginning b) Intermediate c) End

Figure 3: Heat release rate per reaction for a rich H_2-NO_2/N_2O_4(-Ar) mixture with Φ=1.2 at low pressure. $P_0 = 5000$ Pa and $T_0 = 300$ K.

3 Two-dimensional detonation structure

The corresponding two-dimensional simulations carried out are governed by the inviscid Euler equations of motion, i.e. the conservation of mass, momentum, total energy, and chemical species,

$$\begin{aligned} &\frac{\partial \rho}{\partial t} + \nabla \cdot (\rho \boldsymbol{u}) = -\rho \dot{\sigma}_A; \quad \frac{\partial (\rho \boldsymbol{u})}{\partial t} + \nabla \cdot (\rho \boldsymbol{u} \otimes \boldsymbol{u}) + \nabla P = -\rho \boldsymbol{u} \dot{\sigma}_A; \\ &\frac{\partial (\rho E)}{\partial t} + \nabla \cdot \Big((\rho E + P) \boldsymbol{u} \Big) = (\rho E + P) \dot{\sigma}_A; \quad \frac{\partial (\rho Y_i)}{\partial t} + \nabla \cdot (\rho \boldsymbol{u} Y_i) = -\rho Y_i \dot{\sigma}_A + \dot{\omega}_i. \end{aligned} \tag{4}$$

Here, $\boldsymbol{u}$, E, and Y_i are the velocity vector, specific total energy, and mass fraction of the ith species. Following the approach used in the weakly-curved one-dimensional simulations, the impact of boundary layer losses in the third dimension is accounted for through the source terms $\dot{\sigma}_A$ [9, 12]. Here, we approximate the source term using Mirels' boundary layer theory, following the approach of Xiao et al. [9], i.e.

$$\dot{\sigma}_A \approx \frac{K_M}{w} \sqrt{\frac{\nu_s}{t - t_s}}, \tag{5}$$

Here $(t - t_s)$ is the elapsed time since the fluid element crossed through the shock front, see Smith et al. [12] for details. In this two-dimensional planar arrangement, we consider w as a characteristic channel width in the lateral third dimension. Assuming w is small compared to the channel height, an equivalent hydraulic diameter corresponding to the experimental tube diameter [7], can be related to an equivalent width, w, through $D_H \approx 2w$.

The computational domain simulated here was 0.5 m long and 0.04 m high. A slip wall boundary condition was applied to the left boundary, which is suitable for the inviscid framework used. We note that this boundary condition would not influence the detonation wave evolution anyways, since expansion waves originating from it cannot reach the detonation front. A zero gradient boundary condition was applied to the right boundary. The top and bottom boundaries were given periodic boundary conditions. The quiescent fluid at $x > 0$ was at $T_0 = 300$ K and initial pressures of 30 and 100 kPa. The flow field was initialized with the theoretical ZND profile for $-8 < x < 0$ mm, with random perturbations to the density field just in front of the wave to encourage cellular development. The reduced H_2-NO_2/N_2O_4 mechanism composed of 23 species and 20 reactions, proposed by [5], was employed. Details of the numerical methods applied are detailed elsewhere [12], although we do note here that adaptive mesh refinement (AMR) [15] was used to accurately capture areas of interest such as shocks and reaction zones while permitting a lower mesh resolution elsewhere throughout the domain.

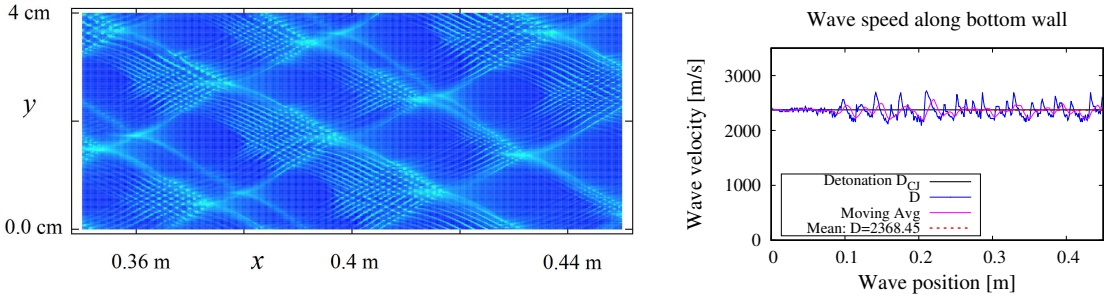

Figure 4: Numerical analysis of soot traces and velocity evolution in a tube at $P_0 = 100$ kPa for a rich H_2-NO_2/N_2O_4-Ar mixture, with an initial temperature $T_0 = 300$ K.

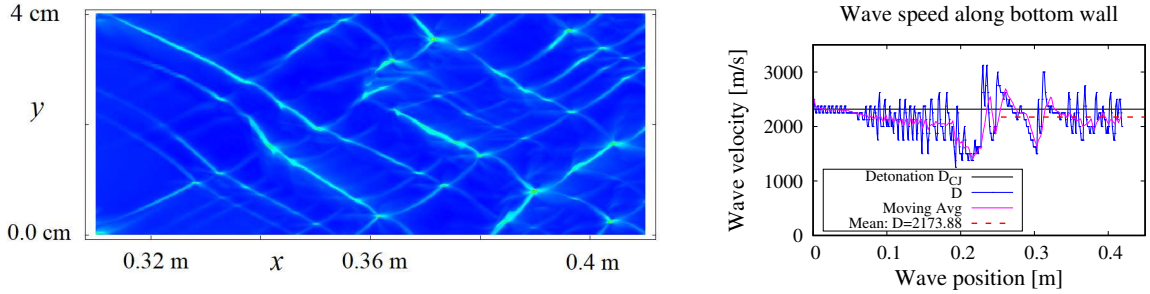

Figure 5: Numerical analysis of soot traces and velocity evolution in a tube at $P_0 = 30$ kPa for a rich H_2-NO_2/N_2O_4-Ar mixture, with an initial temperature $T_0 = 300$ K.

For our preliminary 2-D simulations, initial pressures of $P_0 = 100$ and 30 kPa were considered. Given the high computational cost required to handle the two steps of heat release, the finest grid resolutions obtained were set at 31.25 μm for $P_0 = 100$ kPa, and at 125 μm for $P_0 = 30$ kPa. Therefore, the effective resolution was 2 pts/Δ_1 and 31 pts/Δ_2 at 100 kPa, and 2 pts/Δ_1 and 33 pts/Δ_2 at 30 kPa, where Δ_1 and Δ_2 refer to the induction periods of each exothermic heat release stage. We note that in the Euler framework, cellular structures are likely influenced by changes in the resolution. Here, we aim to provide sufficient resolution in order to capture both the inner and outer structure simultaneously. However, future investigation will examine more closely the influence of resolution on the cellular structures. Figure 4 and Figure 5 respectively show the numerical soot foils and velocity curves obtained under high- and low-pressure conditions. At $P_0 = 100$ kPa, the average velocity is within 1% of D_{CJ}, the theoretical velocity, and agrees well with the value from the weakly-curved simulation. Relatively high-frequency velocity oscillations are observed, and might be related to the dynamics of the cellular structure, which is composed of large cells, with a width on the order of 20 mm, and of much smaller cells, with a width on the order of 1 mm or less. Both cellular networks appear relatively regular. The small cells are mainly located within the last third of the large cell lengths. Given the low effective resolution at D_{CJ} for Δ_1, it should be expected that the small cells become visible only when the average velocity of the leading shock drops below D_{CJ}, i.e., within the last part of a cellular cycle. The soot foil shown in Figure 4 should be interpreted as an under-resolved double cellular structure. Therefore, the numerical results appear to be consistent with the experimental results obtained by Virot et al. [7] under high-pressure conditions. Under low-pressure conditions, the velocity profile demonstrates much larger oscillations, and seems to stabilize around an average velocity of approximately 2170 m/s. This velocity is 70 m/s lower than the experimental value, and represents a velocity deficit of 7% compared to D_{CJ}. At such an initial pressure, the weakly-curved model predicts a velocity 100 m/s higher. The corresponding cellular structure appears quite different compared to the structure observed in the high-pressure case.

It is much more irregular and potentially exhibits sub-structures. In addition, the small network of cell located at the end of the large cell are not present anymore. These features appear qualitatively consistent with the highly irregular, single cellular structures observed by Virot et al. [7] in the low-pressure regime. However, we note that a larger domain height may be needed to capture the outer scale structure.

4 Conclusion

The weakly-curved detonation model has been applied to a rich H_2-NO_2/N_2O_4 mixture which demonstrates a non-monotonous heat release profile. The model can predict well the experimental velocity in the high-velocity regime, but fails in capturing the evolution of the velocity in the low-velocity regime. On the other hand, preliminary 2-D numerical simulations that include flow divergence through a laminar BL model agree qualitatively well with the experimental behavior reported in the literature. At high pressure, a very low velocity deficit and a double cellular structure are observed. At low pressure, a significant velocity deficit and an irregular single cellular structure are observed. While the present 2-D simulations results appear qualitatively consistent with the available experimental observations, it is acknowledged that under-resolved solutions were obtained. Future work will focus on performing numerical simulations with much higher resolutions.

This work is supported by the Natural Sciences and Engineering Research Council of Canada (NSERC), funding reference number RGPIN-2023-03691. Computational resources have also been provided by the Digital Research Alliance of Canada Resources for Research Groups (RRG) 2024 grant, ID 4980. BM acknowledges additional support from UL Research Institutes.

References

[1] Joubert F, Desbordes D, Presles HN. (2008). Detonation cellular structure in NO_2/N_2O_4–fuel gaseous mixtures. Combust. Flame 152:482.

[2] Luche J, Desbordes D, Presles HN. (2006). Détonation de mélanges H_2-NO_2/N_2O_4-Ar. C. R. - Mec. 334:323.

[3] Guilly V, Khasainov B, Presles HN, Desbordes D. (2006). Simulation numérique des détonations à double structure cellulaire. C. R. - Mec. 334:679.

[4] Sugiyama Y, Matsuo A. (2011). On the characteristics of two-dimensional double cellular detonations with two successive reactions model. Proc. Combust. Inst. 33:2227.

[5] Davidenko D, Mével R, Dupré G. (2011). Numerical study of the detonation structure in rich H_2-NO_2/N_2O_4 and very lean H_2-N_2O mixtures. Shock Waves 21:85.

[6] Desbordes D, Presles HN, Joubert F, Douala CG. (2004). Etude de la détonation de mélanges pauvres H_2-NO_2/N_2O_4. C. R. - Mec. 332:993.

[7] Virot F, Khasainov B, Desbordes D, Presles HN. (2010). Two-cell detonation: losses effects on cellular structure and propagation in rich H_2-NO_2/N_2O_4-Ar mixtures. Shock Waves 20:457.

[8] Weng Z, Veiga-López F, Melguizo-Gavilanes J, Mével R. (2023). Effect of ozone addition on curved detonations. Combust. Flame 247:112479.

[9] Xiao Q, Weng C. (2023). Unified dynamics of hydrogen-oxygen-diluent detonations in narrow confinements. Fuel 334:126661.

[10] Ermolaev BS, Khasainov BA, Presles HN, Vidal P. (2005). A simple approach for modelling reaction rates in shocked multi-component solid explosives. Proc. of the European Combustion Meeting.

[11] El Messoudi A, Vidal P, Busegnies Y. (2007). Low-velocity regimes of thermonuclear detonations in type-Ia supernovae,Régimes basse-vitesse de détonations thermonucléaires dans les supernovae de type Ia. C. R. - Mec. 335:768.

[12] Smith J, Schmitt C, Xiao Q, Maxwell B. (2024). On the nature of transverse waves in marginal hydrogen detonation simulations using boundary layer loss modeling and detailed chemistry. Combust. Flame 268:113598.

[13] Xiao Q, Radulescu MI. (2020). Dynamics of hydrogen-oxygen-argon cellular detonations with a constant mean lateral strain rate. Combust. Flame 215:437.

[14] Kao S, Shepherd JE. (2008). Numerical solution methods for control volume explosions and ZND detonation Structure. GALCIT Report FM2006. 7:1.

[15] Falle SAEG, Giddings JR. (1993). Body capturing using adaptive Cartesian grids. Numerical Methods for Fluid Dynamics. Oxford University Press (ISBN 0-198-53696-8).